3. Fe(II) photoautotrophy under a H_2 atmosphere: implications for Banded Iron Formations

ABSTRACT

Both H_2 and Fe(II) can serve as electron donors for anoxygenic photosynthesis and are predicted to have been present in the atmosphere and ocean of the Archean in quantities sufficient for energy metabolism. If H_2, given its more favorable redox potential, is the preferred substrate for anoxygenic phototrophs, this may preclude the involvement of phototrophs capable of Fe(II) photoautotrophy in Banded Iron Formation (BIF) deposition. Here we investigate the effect of H_2 on Fe(II) oxidation by cell suspensions of two strains of Fe(II)-oxidizing purple non-sulfur bacteria. We find that Fe(II) oxidation still proceeds under an atmosphere containing ~3 times the maximum predicted concentration of H_2 in the Archean when CO_2 is abundant. Additionally, the amount of H_2 dissolved in a 100 m photic zone of Archean ocean over an area equivalent to the Hamersley basin may have been less than 0.24 ppm. Therefore, H_2 would pose no barrier to Fe(II) oxidation by ancient anoxygenic phototrophs at depth in the photic zone and would not have precluded the involvement of these bacteria in BIF deposition.

INTRODUCTION

Recent debates in the literature have called into question the idea that evidence for the earliest life in the rock record can be inferred from morphology [23, 148] or chemical composition alone [59, 107, 121]. The value of a search strategy that considers not only morphology and chemical analyses (*e.g.,* isotopic compositions or REE (rare earth element) analyses), but also the ecophysiological context of the fossils in question is becoming increasingly appreciated. An illustration of the power of such a search strategy comes from a recent analysis of the carbonaceous laminations preserved in the shallow water facies of the 3.4 billion year old (Ga) Buck Reef Chert in South Africa [171]. In this work, a synthesis of data from the morphology of the mats as well as sedimentological, petrographic and geochemical investigations allowed for a reconstruction of the environmental setting in which these mat structures were found. This ecological reconstruction enabled the authors to convincingly argue that the mats found in this chert were formed in a euphotic zone that was anoxic, and conclude that the organisms that formed the mats were likely anoxygenic phototrophs, rather than oxygenic.

Further, the authors found a lack of ferric oxide or ferrous sulfide minerals present in the depositional environment of these mats. H_2, however, is thought to have been present in the Archean atmosphere at concentrations between 1000 and 300,000 ppm as a result of volcanic emissions and atmospheric photochemistry [33, 90, 170]. Given the paucity of possible electron donors for photosynthesis in the depositional environment of this ancient mat, Tice and

Lowe deduced that these anoxygenic phototrophs likely used H_2 as their electron donor for carbon fixation, rather than Fe(II) or S^{2-} and thus, H_2-based photoautotrophy was the active metabolism in this environment [111].

In ancient environments where the chemistry is more complex, however, can the dominant active physiologies still be inferred? To address such questions, knowledge concerning the molecular mechanisms of how a particular physiology of interest is regulated must be taken into account. For example, it has been suggested that anoxygenic photoautotrophs able to use ferrous iron [Fe(II)] as an electron donor for photosynthesis were involved in the deposition of the Banded Iron Formations (BIFs) that appear in the rock record prior to the advent of atmospheric O_2 [67, 101, 182]. This model assumes that these bacteria used Fe(II) as an electron donor for photosynthesis; however, if the atmosphere of the early Earth contained quantities of H_2 sufficient to support H_2-based photoautotrophy, would H_2, given its more favorable redox potential [113], be preferred over Fe(II)? If so, would this diminish the likelihood that these bacteria were involved in BIF deposition in certain environments? Coupling an understanding how Fe(II) based photoautotrophy is regulated with biogeochemical/ecological reconstructions of environmental setting can help refine models that consider whether these phototrophs could have catalyzed BIF deposition.

A key assumption that we must make to integrate such physiological and geological information, however, is that the activities of modern organisms are representative and comparable to those of ancient organisms and this

assumption is accepted as a necessary one in this field [3]. Recent studies of the isotopic record of sedimentary sulfides where such assumptions were made have given new insights into when microbial sulfate reduction evolved and the concentrations of sulfate and O_2 in the early Archean ocean and atmosphere [31, 153]. In addition, carbon isotopic studies have revealed traces of autotrophy in the rock record [99, 142, 143]

Here, making the assumption that Fe(II) phototrophy is an ancient metabolism [41] and that extant organisms capable of this metabolism are representative of their ancient relatives, we investigate the effects of H_2 on the Fe(II) oxidation activity of two strains of Fe(II)-oxidizing purple non-sulfur anoxygenic phototrophs and show that Fe(II) oxidation can occur in the presence of H_2 under conditions broadly similar to an Archean ocean.

EXPERIMENTAL PROCEDURES

Organisms and Cultivation

Rhodobacter sp. strain SW2 (SW2) was a gift from F. Widdel (MPI, Bremen, Germany) and *Rhodopseudomonas palustris* strain TIE-1 (TIE-1) was isolated in our lab [83]. Cultures were maintained in a previously described anoxic minimal salts medium for freshwater cultures [52] and were incubated 20 to 30 cm from a 34 W tungsten, incandescent light source at 30°C for TIE-1 and 16°C for SW2. Electron donors for photosynthetic growth were added to the basal medium as follows: thiosulfate was added from an anoxic filter sterilized stock to a final concentration of 10 mM and H_2 was provided as a headspace of

80% H_2: 20% CO_2. For growth on Fe(II), 4 mls of a filter sterilized, anoxic 1 M Fe(II)$Cl_2 \cdot H_2O$ stock solution was added per 1 liter (L) of anaerobic, basal medium (final concentration ~4 mM). To avoid the precipitation of ferrous Fe minerals that results upon addition of Fe(II)$Cl_2 \cdot H_2O$ to the bicarbonate buffered basal medium and the precipitation of ferric Fe minerals that form during the growth of these bacteria on Fe, the metal chelator, nitrilotriacetic acid (NTA, disodium salt from Sigma), was supplied from a 1 M filter sterilized stock solution to a final concentration of 10 mM. This NTA addition greatly facilitated the harvesting of cells, free of Fe minerals, from Fe(II) grown cultures.

Cell suspension assays

All cell suspension assays were prepared under anoxic conditions in an anaerobic chamber (Coy Laboratory Products, Grasslake, MI) to minimize exposure of the cells to oxygen. Cells of SW2 or TIE1 grown on H_2, thiosulfate, or Fe(II)-NTA were harvested in exponential phase (OD_{600} ~0.15 to 0.18) by centrifugation (10,000 rpm on a Beckman JLA 10.5 rotor for 20 min). Pellets were washed once with an equal volume of 50 mM Hepes buffer containing 20 mM NaCl at pH 7 (assay buffer) to remove residual medium components and resuspended in assay buffer containing the appropriate amount of $NaHCO_3$ and Fe(II)$Cl_2 \cdot H_2O$ to a final OD_{600} of 0.1. Resuspending the cells to the same final OD_{600} ensured that the assays were normalized to cell number, as verified by cell counts using a Petroff-Hauser counting chamber. Concentrations of $NaHCO_3$ were 1 or 20 mM and concentrations of Fe(II) were 0.5, 1 or 2 mM. When

appropriate, the protein synthesis inhibiting antibiotic, gentamicin, was added to a final concentration of 0.1, 0.2, 0.5, 1, 2, 4 mg/ml. Unless otherwise stated, assay volumes were 3 mls and cell suspensions of TIE1 and SW2 were incubated at 30°C and 16°C, respectively, in 12 ml stoppered serum bottles at 30 cm from a 34 W tungsten incandescent light bulb. The headspace of the assay bottles contained either 80% N_2:20% CO_2 or 80% H_2:20% CO_2 depending on the particular experiment (see results and figure legends for specific details).

Analytical methods

Fe(II) and Fe(III) concentrations were measured in triplicate by the *Ferrozine* assay [159]. 10 µl of cell suspension was added to 90 µl of 1 N HCL to which 100 µl of *Ferrozine* solution (1 g of *Ferrozine* plus 500 g of ammonia acetate in 1 L of ddH_2O) was added. After 10 minutes, the absorbance at 570 nm was read and the concentration of Fe(II) was determined by comparison to Fe(I) standards. To measure hydrogenase activity, benzyl viologen (Sigma) was added to the assay to a final concentration of 5 mM and the reduction of benzyl viologen was measured at 570 nm in duplicate samples. The program MINEQL$^+$ (Environmental Research Software; http://www.mineql.com/homepage.html) was used to calculate the concentrations of the various Fe(II) and NTA species in the phototrophic minimal salts medium (pH 6.8) when 4 mM Fe(II)$Cl_2 \cdot H_2O$ and 20 mM NTA were added. A closed system was assumed, the ionic strength of the solution was not considered, the temperature was set at 25°C and component concentrations were: H_2O, $1*10^0$; H^+, $1.58*10^{-7}$; Ca^{2+}, $3.69*10^{-6}$; Cl^-, $6.97*10^{-3}$;

CO_3^{2-}, 4.79*10^{-6}; Fe^{2+}, 5.73*10^{-8}; K^+, 3.55*10^{-3}; Mg^{2+}, 1.27*10^{-4}; NH_4^+, 5.47*10^{-3}; SO_4^{2-}, 1.81*10^{-3}; $EDTA^{-4}$, 1.36*10^{-14}; NTA^{-3}, 4.5*10^{-6}.

RESULTS AND DISCUSSION

Effects of NTA

The products of Fe(II) oxidation by TIE-1 and SW2 are poorly crystalline ferric (hydr)oxide precipitates [41, 89]. These precipitates greatly hinder our ability to harvest cells for physiological studies. To prevent the precipitation of ferric phases in our cultures, we added varying concentrations of the chelator NTA to our growth medium containing Fe(II) and found that a concentration of at least 10 mM NTA was necessary to keep Fe(III) in solution for both cultures. As has been observed before for the Fe(II)-oxidizing phototrophic strain, *Rhodomicrobium vannielli* [70], the addition of NTA accelerated the rate of Fe(II) oxidation. For TIE-1, the addition of 7.5, 15, and 20 mM NTA increased the Fe(II) oxidation rate approximately 44, 52 and 55%, respectively, and for SW2, the rate increased approximately 22% upon addition of 7.5 or 10 mM of NTA (Figure 3-1A and 1B). The acceleration of Fe(II) oxidation does not result from stimulation of growth by the addition of this organic compound, as control experiments showed that neither TIE-1 nor SW2 could grow on NTA alone (data not shown). In some Fe(II)-oxidizing phototrophs, the ferric precipitate products of this form of metabolism completely encrust the cells and impede further oxidation [70]. While such severe consequences of ferric precipitation are not evident with TIE-1 or SW2, it is possible that the deposition of these precipitates

at the surface of the cell does have inhibitory effects of the rate of Fe(II) oxidation. Given this, an alternative explanation for the increased rate of Fe(II) oxidation upon addition of NTA may be that solubilization of the ferric precipitates alleviates product inhibition of this metabolism by these precipitates.

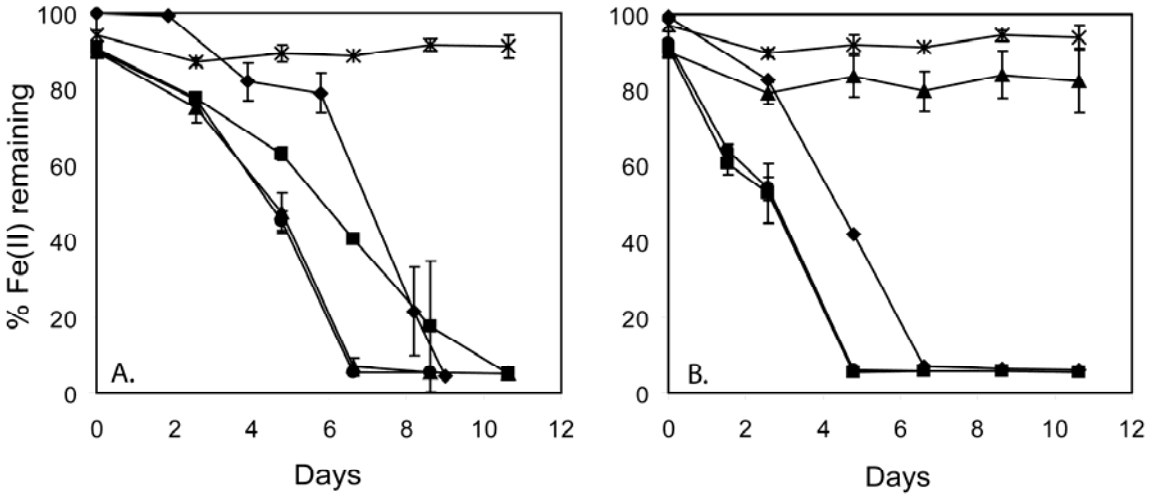

Figure 3-1: Growth of TIE-1 and SW2 on 4 mM Fe(II)$Cl_2 \cdot H_2O$ + varying concentrations of NTA. A. Data for TIE-1: ♦ - 0 mM NTA, ■ - 7.5 mM NTA, ▲ - 15 mM NTA, ● - 20 mM NTA, ✳ - Abiotic + 20 mM NTA. B. Data for SW2: ♦ - 0 mM NTA, ■ - 7.5 mM NTA, ● - 10 mM NTA, ▲ - 15 mM NTA, ✳ - Abiotic + 20 mM NTA. No growth was observed in cultures of TIE-1 or SW2 where only NTA and no Fe(II) was added, indicating that these strains cannot use NTA as a substrate for growth. The lower concentration of Fe(II) at time 0 in the cultures where NTA has been added as compared to the cultures with no NTA addition indicates there is a pool of Fe(II) we cannot measure with the *Ferrozine* assay. Error bars represent the error on duplicate cultures.

The concentration of NTA tolerated by the two strains differed. TIE-1 could tolerate up to 20 mM NTA (higher concentrations were not tested) (Figure 3-1A) whereas concentrations higher the 10 mM were inhibitory for SW2 (Figure 3-1B). MINEQL^{+} modeling of the chemical speciation of the medium shows that upon initial addition of 4 mM Fe(II)$Cl_2 \cdot H_2O$ to medium containing 5-20 mM NTA, 99.8% of the total Fe(II) is present as the Fe[NTA] species (Figure 3-2A and 2B and Table 3-1 and 2 for 20 mM NTA). It is, therefore, unlikely that the increased resistance of TIE-1 to NTA, relative to SW2, results from the production of Fe(II) chelators by this strain, because the Fe-NTA speciation remains the same within our tested NTA concentration span. Rather, it may result from a more general mechanism, related perhaps to differences in cell wall permeability or the efficiency/number of generalized solute efflux pumps. This later hypothesis would be consistent with the observation that TIE-1 is resistant to a greater concentration of the antibiotics kanamycin, gentamicin, tetracycline and chloramphenicol (the mechanisms of resistance of the latter two being via efflux) than most purple non-sulfur bacteria on solid and liquid media [83].

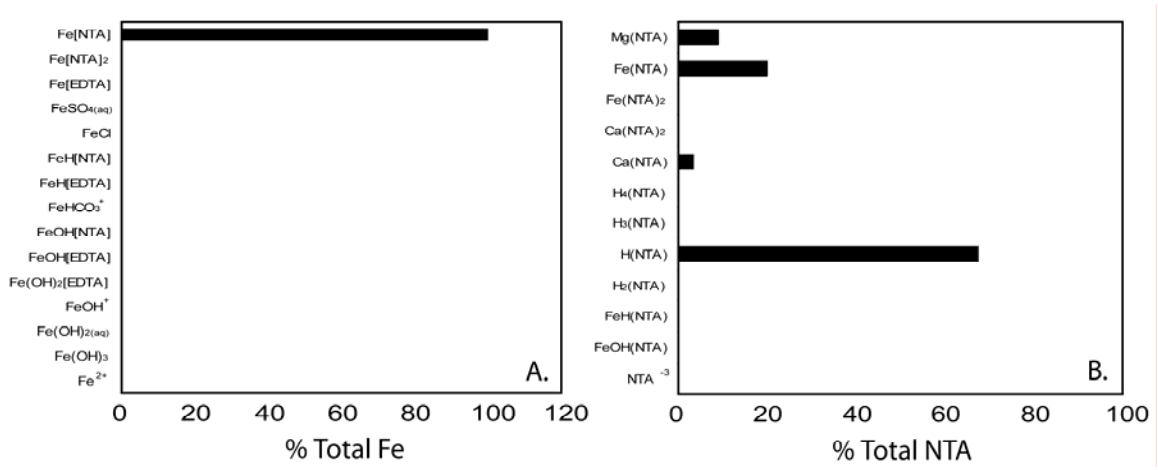

Figure 3-2: Concentrations of A. Fe(II) and B. NTA species in the phototrophic basal medium (pH 6.8). Concentrations are represented as % of total Fe(II) (4 mM $Fe(II)Cl_2 \cdot H_2O$) and NTA (20 mM Na_2NTA) as calculated with MINEQL$^+$. See text for model parameters.

Table 3-1: Molar concentrations the NTA species in the phototrophic basal medium with 4 mM $Fe(II)Cl_2 \cdot H_2O$ and 20 mM NTA at pH 6.8, as calculated with MINEQL$^+$.

NTA species	Molar concentration
FeOH(NTA)	4.50E-06
FeH(NTA)	1.41E-07
H_2(NTA)	7.96E-08
H(NTA)	1.87E-06
H_3(NTA)	1.35E-02
H_4(NTA)	2.97E-11
Ca(NTA)	4.70E-17
$Ca(NTA)_2$	6.73E-04
$Fe(NTA)_2$	4.82E-08
Fe(NTA)	4.82E-06
Mg(NTA)	3.99E-03
Total NTA	2.00E-02

Table 3-2: Molar concentrations of the Fe(II) species in the phototrophic basal medium with 4 mM Fe(II)$Cl_2 \cdot H_2O$ and 20 mM NTA at pH 6.8, as calculated with MINEQL$^+$.

Fe(II) species	Molar concentration
Fe^{2+}	5.73E-08
$Fe(OH)_3$	1.47E-16
$Fe(OH)_{2(aq)}$	7.31E-15
$FeOH^+$	1.45E-10
$Fe(OH)_2$ [EDTA]	3.10E-12
FeOH[EDTA]	1.55E-08
FeOH[NTA]	1.41E-07
$FeHCO_3^+$	1.17E-08
FeH[EDTA]	1.42E-09
FeH[NTA]	7.96E-08
FeCl	2.52E-10
$FeSO_{4(aq)}$	2.54E-08
Fe[EDTA]	7.79E-06
$Fe[NTA]_2$	4.82E-06
Fe[NTA]	3.99E-03
Total Fe(II)	4.00E-03

Fe(II) oxidation under a H_2 atmosphere

A general assumption in bacterial physiology is that electron donors that yield the most energy for growth will be preferred over those that yield less. Thus, in a bicarbonate containing system where the relevant Fe couple, $Fe(OH)_3$ + $HCO_3^-/FeCO_3$, has a redox potential of +0.2 V [52], H_2, with the redox potential of the relevant couple, $2H^+/H_2$, being -0.41 V [113], is expected to be preferred as a source of electrons for growth over Fe(II). This implies that in an environment where H_2 and Fe(II) co-exist, photoautotrophic Fe(II) oxidation may not be a relevant physiology to consider.

Interested in whether the availability of H_2 as an electron donor might inhibit Fe(II) oxidation by ancient relatives of TIE-1 and SW2, we investigated the effects of H_2 on the Fe(II) oxidation activity of these two strains in cell suspension assays where the concentrations of Fe(II), $NaHCO_3$ and H_2 were comparable to those predicted for an ancient Archean ocean. Namely, our initial Fe(II) concentration of ~0.4 to 0.45 mM is within the range of 0.054 to 0.54 mM predicted by Holland and Ewers [57, 72], our $NaHCO_3$ concentration of 20 mM is on the same order as the 70 mM predicted for an Archean ocean and an order of magnitude higher than the present day concentration of 2 mM [65], and our H_2 concentration of 800,000 ppm is also on the same order as the recently proposed concentration in the early atmosphere of 300,000 ppm [170].

In our experiments containing 1 mM $NaHCO_3$, in the absence of H_2, we observed initial rates of Fe(II) oxidation for TIE-1 and SW2 of 0.07 mM/hr and 0.15 mM/hr, respectively (Figure 3-3A and 3B, Table 3-3). Under the same low $NaHCO_3$ conditions, in the presence of H_2, the rate of Fe(II) oxidation by TIE-1 decreased by 44% as compared to the absence of H_2 (Figure 3-3A, Table 3-3). SW2, however, showed a much more dramatic inhibition by H_2 under low $NaHCO_3$ conditions. Here, the rate of Fe(II) oxidation decreased to 0.03 mM/hr during the first 5 hours (78% of the rate in the absence of H_2) and further decreased to 0.01 (on average) thereafter, resulting in only 22% of the total Fe(II) being oxidized within the 10 hour course of the experiment (Figure 3-3B, Table 3-3).

Under 20 mM $NaHCO_3$, however, while the rates of Fe(II) oxidation in the presence of H_2 decreased for the two strains, we did not observe such dramatic decreases, as compared to the 1 mM $NaHCO_3$ conditions. For TIE-1, in the presence of H_2 the initial rate of Fe(II) oxidation decreased 26% as compared to the rate of oxidation in absence of H_2 (Figure 3-3A, Table 3-3). For SW2 the initial rate of Fe(II) oxidation decreased 39% when H_2 is present (Figure 3-3B, Table 3-3). Regardless of the slight decreases in Fe(II) oxidation rate in the presence of H_2, however, for SW2, all of the Fe(II) is oxidized to completion within 2 hours and for TIE-1, after 8 hours, the same amount of Fe(II) is oxidized as in the absence of H_2 (Figure 3-3A and 3B).

These results indicate that Fe(II) oxidation by some anoxygenic phototrophs may be severely inhibited by the presence of H_2 in modern environments where the concentration of $NaHCO_3$ is low (2 mM). However, if the concentration of $NaHCO_3$ is high (*i.e.*, at least 20 mM), as is assumed to be the case in an Archean ocean, even in the presence of H_2, Fe(II) oxidation by these phototrophs could still have proceeded at appreciable, although slightly reduced, rates. Further, these results demonstrate that the utilization of substrates may change under different conditions and the co-utilization of substrates during anoxygenic photosynthesis is possible. Substrate preference must, therefore, be experimentally demonstrated under the particular conditions of interest.

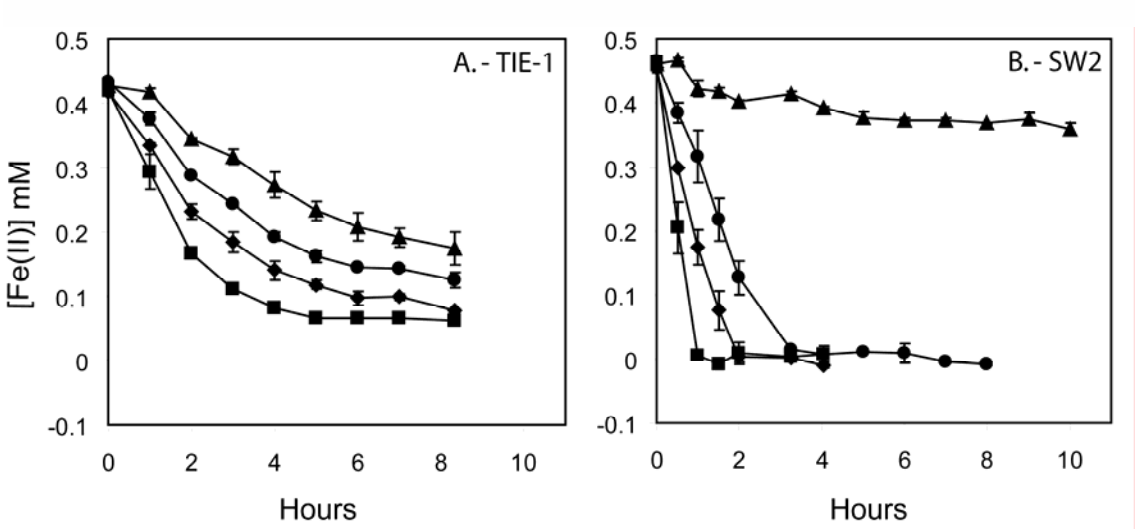

Figure 3-3: H_2 inhibits the Fe(II) oxidation activity of both TIE-1 and SW2 to varying degrees depending on the concentration of $NaHCO_3$. A. Data for TIE-1: ▲ - H_2 + 1 mM $NaHCO_3$ + 0.5 mM $FeCl_2 \cdot H_2O$; ● - N_2 + 1 mM $NaHCO_3$ + 0.5 mM $FeCl_2 \cdot H_2O$; ♦ - H_2 + 20 mM $NaHCO_3$ + 0.5 mM $FeCl_2 \cdot H_2O$; ■ - N_2 + 20 mM $NaHCO_3$ + 0.5 mM $FeCl_2 \cdot H_2O$. B. Data for SW2: ▲ - H_2 + 1 mM $NaHCO_3$ + 0.5 mM $FeCl_2 \cdot H_2O$; ● - N_2 + 1 mM $NaHCO_3$ + 0.5 mM $FeCl_2 \cdot H_2O$; ♦ - H_2 + 20 mM $NaHCO_3$ + 0.5 mM $FeCl_2 \cdot H_2O$; ■ - N_2 + 20 mM $NaHCO_3$ + 0.5 mM $FeCl_2 \cdot H_2O$. Data are representative of at least two independent experiments. The volume of the assay was 1 ml and the assay bottles were shook vigorously to ensure maximal H_2 saturation of the cell suspension solution. Error bars represent the error on duplicate cell suspension assays for TIE-1 and triplicate assays for SW2.

Table 3-3: Rates of Fe(II) oxidation by cell suspensions of TIE-1 and SW2. The rate of Fe(II) oxidation for the TIE-1 + H_2/CO_2 + 1 mM $NaHCO_3$ + 0.5 mM Fe(II)$Cl_2 \cdot H_2O$ assay was calculated using the first four time points, all others were calculated using the first three time points. The rate of Fe(II) oxidation for the SW2 + H_2/CO_2 + 1 mM $NaHCO_3$ + 0.5 mM $FeCl_2 \cdot H_2O$ assay was calculated using the first five time points, all others were calculated using the first three time points.

Assay Condition	mM Fe(II) oxidized/hour	R^2	% decrease in rate relative to no H_2 conditions
TIE-1 + H_2/CO_2 + 1 mM $NaHCO_3$ + 0.5 mM $FeCl_2 \cdot H_2O$	0.04	0.93	44
TIE-1 - N_2/CO_2 + 1 mM $NaHCO_3$ + 0.5 mM $FeCl_2 \cdot H_2O$	0.07	0.99	
TIE-1 + H_2/CO_2 + 20 mM $NaHCO_3$ + 0.5 mM $FeCl_2 \cdot H_2O$	0.09	1	26
TIE-1 - N_2/CO_2 + 20 mM $NaHCO_3$ + 0.5 mM $FeCl_2 \cdot H_2O$	0.13	1	
SW2 - H_2/CO_2 + 1 mM $NaHCO_3$ + 0.5 mM $FeCl_2 \cdot H_2O$	0.03 – first 2 hours 0.01 – 2 to 10 hours	0.86 0.71	78
SW2 - N_2/CO_2 + 1 mM $NaHCO_3$ + 0.5 mM $FeCl_2 \cdot H_2O$	0.15	1	
SW2 + H_2/CO_2 + 20 mM $NaHCO_3$ + 0.5 mM $FeCl_2 \cdot H_2O$	0.28	1	39
SW2 - N_2/CO_2 + 20 mM $NaHCO_3$ + 0.5 mM $FeCl_2 \cdot H_2O$	0.45	1	

Inferences on the mechanism of Fe(II) oxidation inhibition by H_2

The molecular mechanism by which H_2 inhibits Fe(II) oxidation is not understood. Cell suspensions of TIE-1 and SW2 cells incubated in the dark show that all the Fe(II) oxidation activity observed in H_2 pre-grown cells is light dependent (Figure 3-4).

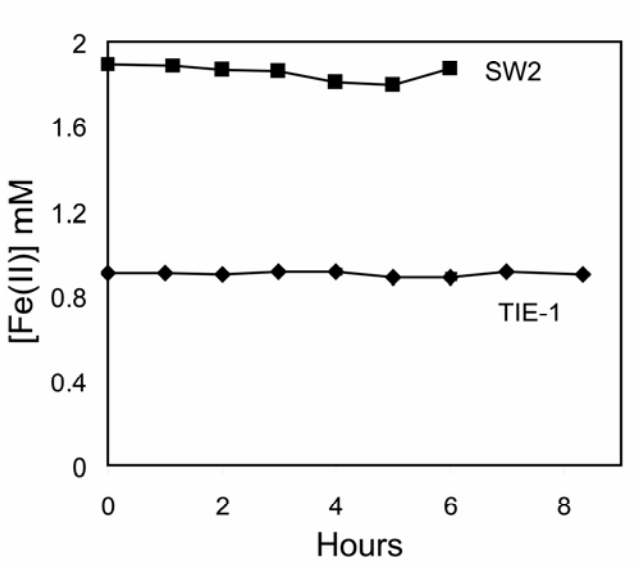

Figure 3-4: The Fe(II) oxidation activity of cell suspensions of TIE-1 and SW2 is completely light dependent. ♦ - H_2 pre-grown TIE-1 cells + N_2 + 20 mM $NaHCO_3$ + 1 mM $FeCl_2 \cdot H_2O$, incubated in the dark. ■ - H_2 pre-grown SW2 cells + N_2 + 20 mM $NaHCO_3$ + 2 mM $FeCl_2 \cdot H_2O$, incubated in the dark.

This implies that electron flow from Fe(II) is specific to the photosynthetic electron transport system. If the same is true for electrons derived from H_2, there exist a number of possibilities by which H_2 might inhibit Fe(II) oxidation. These possibilities include: 1) Hydrogenase, the enzyme that oxidizes H_2, delivering the

electrons to the photosynthetic electron transport chain at the level of the quinone pool [178], is the same enzyme that oxidizes Fe(II) and this enzyme has a higher affinity or faster rate of reaction with H_2 than Fe(II). If the enzyme that oxidizes Fe(II) (Fe oxidase) is not the hydrogenase enzyme, 2) H_2 may inhibit the expression of the Fe(II) oxidase, 3) H_2 may directly inhibit the Fe(II) oxidase itself, or 4) hydrogenase is active in these cells and is effectively out-competing the Fe(II) oxidase to donate electrons to the photosynthetic electron transport chain.

Although the formal possibility exists that the Fe(II) oxidase and the hydrogenase are the same enzyme, this seems highly unlikely given the very different redox potentials and molecular structures of these substrates. Moreover, there is no precedent in the literature for a hydrogenase with Fe(II) oxidation activity. In addition, if the hydrogenase enzyme catalyzes Fe(II) oxidation, cells pre-grown on H_2 would be expected to have greater Fe(II) oxidation activity than cells pre-grown on thiosulfate, as less hydrogenase would be expressed when H_2 is not present to induce its expression [178]. Cells pre-grown on thiosulfate, however, show a rate of Fe(II) oxidation equivalent to cells pre-grown on H_2 (Figure 3-5).

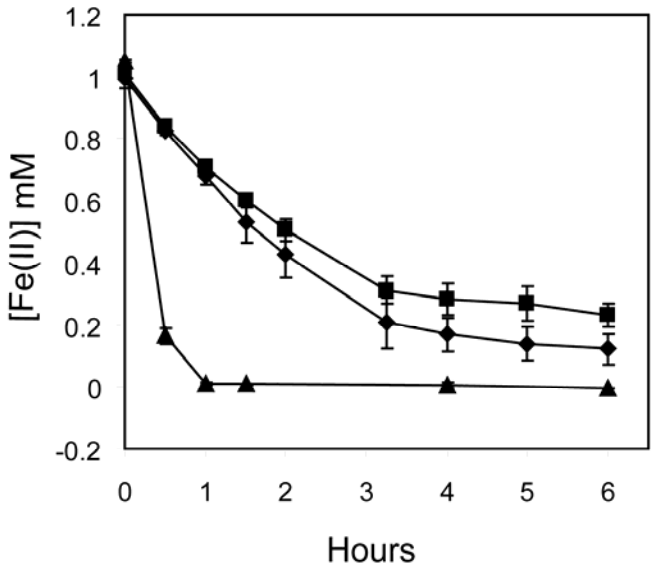

Figure 3-5: Fe(II) oxidation activity of cell suspensions of TIE-1 pre-grown photoautotrophically on different inorganic electron donors. ■ - TIE-1 pre-grown on 10 mM thiosulfate, ♦ - TIE-1 pre-grown on H_2, ▲ - TIE-1 pre-grown on 4 mM $FeCl_2 \cdot H_2O$ + 10 mM NTA. Cells used in this assay were normalized for cell number and the error bars represent the error on triplicate cell suspension assays.

Interestingly, cells pre-grown on Fe(II)-NTA show a greater rate of Fe(II) oxidation than those pre-grown on thiosulfate or H_2 (Figure 3-5). This shows that components necessary for Fe(II) oxidation are expressed to varying degrees under different conditions and implies that their expression is inducible. Further, evidence for the inducible nature of this activity comes from cell suspension assays conducted on H_2 pre-grown cells where the protein synthesis gentamicin was added at increasing concentrations. Here, the Fe(II) oxidation activity decreased with increasing concentration of gentamicin (Figure 3-6).

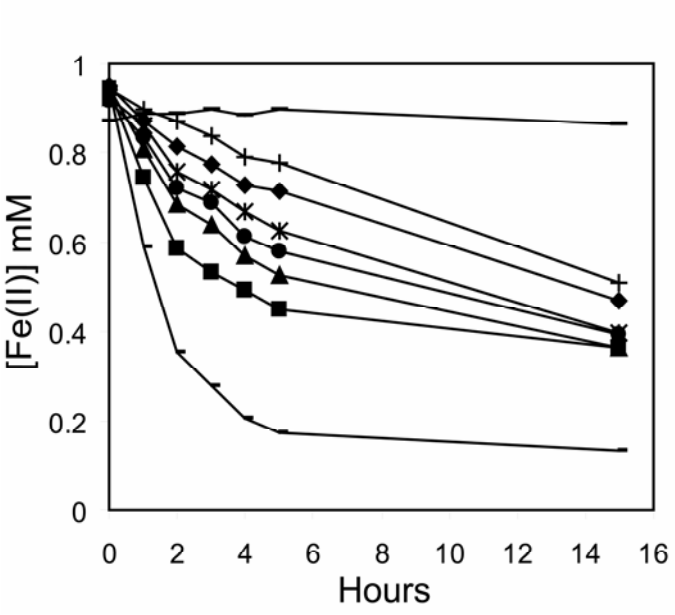

Figure 3-6: The Fe(II) oxidation activity of H_2 pre-grown cells of TIE-1 decreases with increasing concentration of gentamicin. All assays here contain 1 mM $FeCl_2 \cdot H_2O$ and 20 mM $NaHCO_3$. – (short dash) - no gentamicin added; ■ - 0.1 mg/ml gentamicin; ♦ - 0.2 mg/ml gentamicin; ▲ - 0.5 mg/ml gentamicin; ● - 1 mg/ml gentamicin; + - 2 mg/ml gentamicin; ✳ - 4 mg/ml gentamicin; — (long dash) abiotic control + 4 mg/ml gentamicin.

If gentamicin is acting to inhibit novel protein synthesis as expected, these results show that new protein synthesis must be induced and is required for maximal Fe(II) oxidation activity under our assay conditions. The factors that induce this activity are currently unknown, however, based on analogy to the hydrogenase and the sulfide quinone reductase enzymes (the enzyme responsible for the oxidation of S^{2-} during photoautotrophic growth on S^{2-} in many purple non-sulfur phototrophs) [64, 178], it is likely that the Fe(II) oxidase is induced to some level by its substrate, Fe(II).

Assuming that Fe(II) and H_2 oxidation are catalyzed by different enzymes, if H_2 inhibits expression of the Fe(II) oxidase or the Fe(II) oxidase enzyme itself, cells pre-grown on H_2 and transferred to assay conditions containing both Fe(II) and H_2 would be expected to have no Fe(II) oxidation activity (during H_2 pre-growth the Fe(II) oxidase would be repressed and upon transfer to the assay containing H_2, the repression of the Fe(II) oxidase would continue due to the presence of H_2). On the contrary, in our experiments where we add H_2 to the assay to investigate its effects on Fe(II) oxidation, we see that the cells do have Fe(II) oxidation activity (albeit, less than the activity observed for H_2 pre-grown cells transferred to an assay with only Fe(II) (Figure 3-3A and 3B). This observation implies that the Fe(II) oxidase can be expressed in the presence of H_2 and thus, is not repressed transcriptionally, or post-translationally by H_2, itself.

This leaves us to consider the possibility that the observed inhibition of Fe(II) oxidation by H_2 results from the fact that both the hydrogenase and Fe(II) oxidase enzymes are present and active under our assay conditions and compete to donate electrons to the photosynthetic electron transport chain and ultimately CO_2; the implication of this being that the electrons from H_2 out-compete those from Fe(II).

The flow of electrons from Fe(II) and H_2 to the photosynthetic electron transport chain and CO_2 is shown in Figure 3-7.

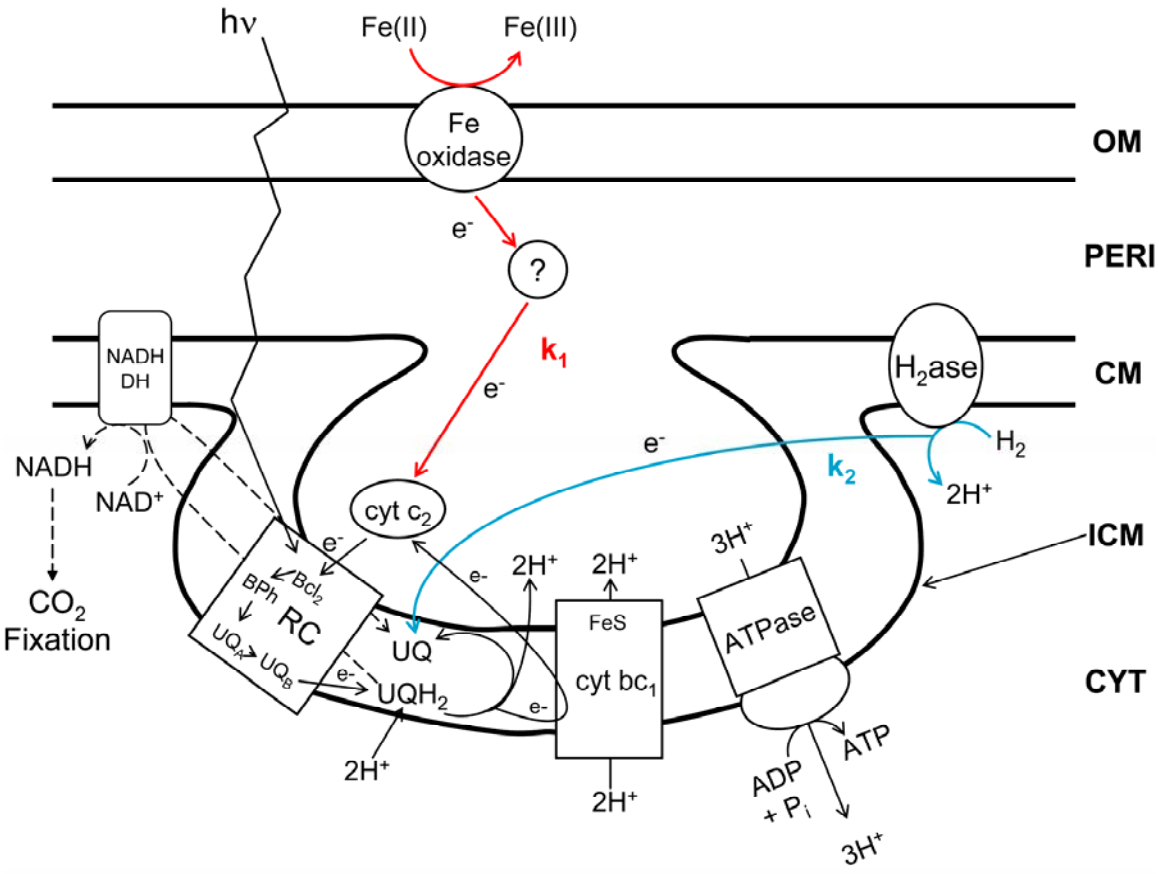

Figure 3-7: A cartoon representation of the flow of electrons from Fe(II) and H_2 to the photosynthetic electron transport chain and CO_2. For simplicity, Fe(II) oxidation is represented as occurring outside the cell. The red lines, associated with k_1, represent the pathway and the overall rate of electron flow from Fe(II) to the photosynthetic electron transport chain. The blue lines, associated with k_2, represent the pathway and the overall rate of electron flow from H_2 to the photosynthetic electron transport chain. OM: outer membrane; PERI: periplasm; CM: cytoplasmic membrane; ICM: intracytoplasmic membrane; CYT: cytoplasm.

The hydrogenase enzyme, presumably located in the cytoplasmic membrane (CM) of TIE-1 and SW2 by comparison to *Rhodobacter capsulatus*

[178], donates electrons from H_2 to the quinone pool. These electrons can then flow through the photosynthetic electron transport chain in a cyclic fashion to produce ATP or feed into NAD^+ reduction (catalyzed by the NADH dehydrogenase also located in the CM). NADH can then be used to fix CO_2.

The location of the Fe(II) oxidase is not yet known. Because Fe(III) formed in the periplasm or cytoplasm would precipitate given the neutral pH at which these organisms grow, it has been proposed that oxidation of Fe(II) occurs at the cell surface and that the electrons are shuttled to the phototrophic reaction center within the intracytoplasmic membrane via a periplasmic transport system involving Cyt c_2 [52]. Alternatively, it is possible that Fe(II) is oxidized internal to the outer membrane (OM). If this is the case, we expect that Fe-chelators (be they organic or inorganic) keep the Fe(III) from precipitating until it can be exported from cell or that subtle changes in local pH control Fe(III) precipitation [41, 89]. In Figure 3-7, the Fe oxidase is depicted as residing in the OM for simplicity. Here, the electrons from Fe(II) flow into the photosynthetic electron transport chain via Cyt c_2 and, as is the case for electrons from H_2, continue to flow through the chain in a cyclic fashion to produce ATP or feed into NAD^+ reduction. Whether intermediate carries between the Fe(II) oxidase and Cyt c_2 also play a role is unknown.

Under conditions where the physiological electron acceptor, CO_2, is abundant (*i.e.*, 20 mM $NaHCO_3$), H_2 inhibition of Fe(II) oxidation is observed as a slight decrease in the rate of Fe(II) oxidation for both TIE-1 and SW2 (Figure 3-3A and 3B, Table 3-3). If these enzymes are competing to donate electrons to

the photosynthetic electron transport chain and ultimately CO_2, when the concentration of the electron acceptor is low (*i.e.*, 1 mM $NaHCO_3$), we might expect the competition between the two enzymes to become more intense and be manifested as a greater inhibition of Fe(II) oxidation by H_2. In support of this hypothesis, we observe that the rate of Fe(II) oxidation for both strains under low $NaHCO_3$ concentrations decreased more so in the presence of H_2 as compared to higher $NaHCO_3$ concentrations, particularly for SW2 (Figure 3-3A and 3B, Table 3-3).

To further test this competition hypothesis, we measured the hydrogenase activity of cell suspensions of TIE-1 pre-grown on H_2 in the presence and absence of Fe(II) to determine if the hydrogenase enzyme is in fact present and active in our assay conditions. The H_2-dependent reduction of benzyl viologen observed indicates that the cells used for our assay do have an active hydrogenase, the activity of which does not seem to be affected by the presence or absence of Fe(II) (Figure 2A & B). These findings are as expected given that the cell are pre-grown on H_2, a condition where the hydrogenase is expected to be highly expressed [178].

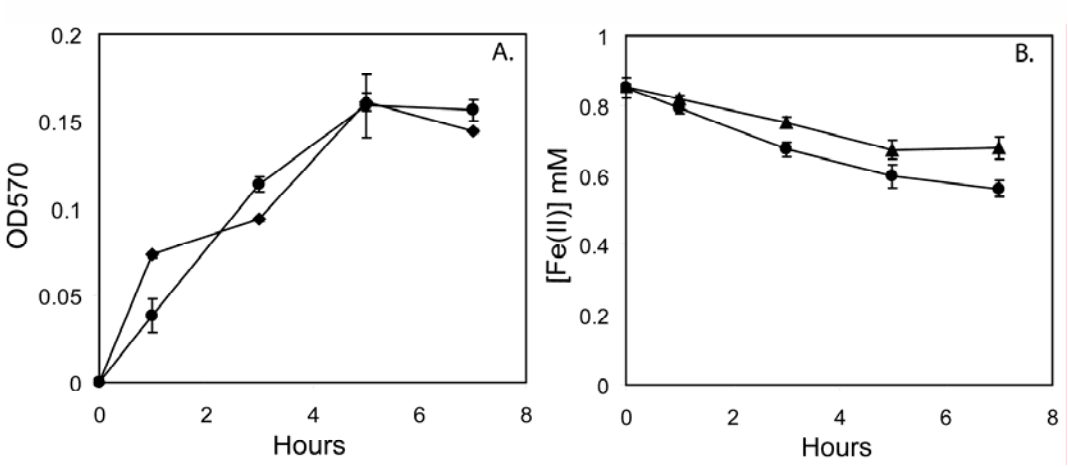

Figure 3-8: Hydrogenase and Fe(II) oxidation activity for TIE-1 as measured by benzyl viologen (BV) reduction and *Ferrozine*, respectively. A. Hydrogenase activity for TIE-1: ♦ - H_2 + 20 mM $NaHCO_3$ + 1 mM $FeCl_2 \cdot H_2O$ + 5 mM BV; ● - H_2 + 20 mM $NaHCO_3$ + 5 mM BV. B. Fe(II) oxidation activity for TIE-1: ▲ H_2 + 20 mM $NaHCO_3$ + 1 mM $FeCl_2 \cdot H_2O$; ● - N_2 + 20 mM $NaHCO_3$ + 1 mM $FeCl_2 \cdot H_2O$. The volume of the assay was 1 ml and the assay bottles were shook vigorously to ensure maximal H_2 saturation of the cell suspension solution. Error bars represent the error on triplicate cell suspension assays.

That the extent of Fe(II) oxidation in the presence of H_2 is limited by the concentration of $NaHCO_3$ in both TIE-1 and SW2 implies that in both strains, the overall rate at which electrons are delivered to the photosynthetic electron transport chain from Fe(II) (k_1, Figure 3-7) is slower than the overall rate at which electrons are delivered to the photosynthetic electron transport chain from H_2 (k_2, Figure 3-7). Reasons why k_2 may be greater than k_1 cannot be determined from our current data, but there are a number of possibilities. First, it is possible that the rate(s) of reaction of the enzymes in the H_2 pathway are faster relative to the

rates of reaction of the enzymes in the Fe(II) pathway. Second, there may be a greater abundance of hydrogenase in these cells relative to the Fe(II) oxidase, which is likely given that these cells are pre-grown on H_2. A final possibility hinges on the fact that that electrons from H_2 are delivered to the photosynthetic electron transport chain via the quinone pool, whereas electrons from Fe(II) are presumably delivered at the level of Cyt c_2. Given that the quinone pool is larger than the Cyt c_2 pool with reported ratios of 20-25 molecules of quinone to each reaction center versus 2 molecules of Cyt c_2 per reaction center [49, 167, 176], the quinone pool represents a larger sink for electrons than the Cyt c_2 pool, and is thus likely to be less limiting in terms of the amount of electrons that can be accepted from the substrate. Further, because the pathway to the NADH dehydrogenase of electrons donated directly to the quinone pool is shorter than that of electrons fed in though the Cyt c_2 pool (which must first go through the reaction center), electrons from H_2 get fed into NAD+ reduction and subsequent CO_2 fixation faster than those from Fe(II). These factors together may serve to accelerate the overall rate of H_2 oxidation relative to Fe(II) oxidation.

The physiological basis for the difference in sensitivity to H_2 under low $NaHCO_3$ concentrations that is observed for the two strains remains to be determined. The greater degree of inhibition by H_2 observed for SW2 relative to TIE-1, however, may imply that k_1 for SW2 is effectively less than k_1 for TIE-1 (Figure 3-7). Such a scenario may result if k_1 is less than k_2 in SW2, whereas k_1 and k_2 are more equivalent in TIE-1, or if there is a greater concentration of hydrogenase relative to Fe(II) oxidase in SW2 versus TIE-1. Such questions

concerning the rates of individual reactions within a physiological pathway cannot be resolved with cell suspension experiments and require further investigations with purified enzymes. Thus, purification of the Fe(II) oxidase is a priority for future work.

Implications for Banded Iron Formations

Inferences on mechanism aside, the implication of our results for Banded Iron Formations are that when the physiological electron acceptor for photosynthesis (CO_2), is abundant (as would be the case in an ancient Achaean ocean) some Fe(II) oxidizing phototrophs have the capacity to oxidize Fe(II) even in the presence of the alternative electron donor, H_2. Thus, the presence of H_2 in an ancient atmosphere up to concentrations of even 800,000 ppm would not necessarily preclude Fe(II) oxidation by these bacteria. That our $NaHCO_3$ concentrations (20 mM) are lower than the predicted concentrations in an Archean ocean by ~3.5 fold implies that the slight inhibitory effects of H_2 observed under our conditions might be negligible at concentrations of 70 mM.

If we assume that photochemical reactions and volcanic emissions were the major source of H_2 and calculate the concentration of H_2 in a photic zone of 100 m over an area of 10^{11} m^2 (equivalent to the depositional basin of the Hamersley Group, which contains among the largest BIFs [101]), using a hydrogen mixing ratio of 30% (which is at the upper limit of what has been predicted [170]), and a Henry's constant for H_2 of $10^{-3.1}$ [122], we find the concentration of H_2 expected in this volume of ocean water to be 0.24 ppm (0.24

mM). Given that diffusion and H_2 consumption rates by other bacteria are not considered in this calculation, we expect the concentration of H_2 to further decrease with depth. Additionally, the solubility of H_2 in water decreases with increasing temperature [60]. If estimations of Archean ocean temperatures at 70±15°C are correct [97], our calculated value represents a maximum for the amount of H_2 dissolved in the photic zone of this basin and is several orders of magnitude less than those used for our experiments. Therefore, it is likely that at depths approaching 100 m in the ancient open ocean, H_2 would pose no barrier to Fe(II) oxidation by these anoxygenic phototrophs. Further, in sulfide depleted environments, which are thought to prevail in the ancient oceans prior to 1.8 Ga [134], Fe(II) may be the predominant inorganic electron donor for anoxygenic photosynthesis in an Archean ocean.

CONCLUSIONS

We find that even in the presence of 800,000 ppm H_2, Fe(II) is still oxidized at appreciable rates by two species of Fe(II)-oxidizing purple non-sulfur phototrophs when the concentration of $NaHCO_3$ is 20 mM. This implies that the presence of H_2 in an ancient atmosphere at the currently predicted values would not preclude the involvement of these organisms in BIF deposition. Additionally, our calculations predict that the concentration of dissolved H_2 in the photic zone of an Archean ocean would be less than 0.24 ppm; a concentration that is expected to have no effect on Fe(II) oxidation by anoxygenic phototrophs at depth in the photic zone. Further, in sulfide depleted environments, which are

thought to prevail in the ancient oceans prior to 1.8 Ga [134], Fe(II) may be the predominant inorganic electron donor for anoxygenic photosynthesis in an Archean ocean.

The molecular mechanism by which H_2 inhibits Fe(II) oxidation by these phototrophs when $NaHCO_3$ concentrations are low remains to be determined, but the most likely explanation appears to be that it results from a competition between hydrogenase and the Fe(II) oxidase to donate electrons to the photosynthetic electron transport chain and ultimately CO_2. The physiological differences between TIE-1 and SW2 that result in differential sensitivity to H_2 are also not known, but the difference may result from different rates of reaction for enzymes in the Fe(II) and/or H_2 oxidation pathways of the two strains.

A consideration that remains to be investigated is the effect that organic compounds may have on phototrophic Fe(II) oxidation. Further studies that combine microbial physiology and the geological approaches that allow biogeochemical reconstructions of ancient environments will help shed light on this and other questions related to BIF deposition and the ecology of the Archean.